Approximate Bridging Relations in the Transitional Regime between Continuum and Free-Molecule Flows

FRED W. MATTING*
NASA Ames Research Center, Moffett Field, Calif.

Approximate bridging relations for aerodynamic quantities in the transitional regime between free-molecule and continuum flows are developed. Equations are presented for heat transfer, surface shear, and drag, and are proposed for lift and pressure distribution. The equations can be considered as semiempirical. They are derived from models based on simplified kinetic theory; the structure of the equations is such that they are asymptotically correct at the free-molecule and continuum extremes, and this tends to place bounds on errors resulting from a simplified analysis. The equations presented are essentially for blunt bodies; that may be used as engineering approximations in many cases for which more rigorously developed specific relations do not exist.

Nomenclature

A = area
A_{cq} = free-molecule accommodation coefficient for heat transfer, dimensionless
C_{cal} = calorimeter constant, Eq. (22)
C_D, C_L = drag and lift coefficients, respectively, dimensionless
C_f = coefficient of local skin friction, dimensionless
C_{vort} = vorticity correction constant, Eq. (22)
C_Δ = constant defined by Eq. (34)
E_D, E_L, E_p = body shape factor for drag, lift, pressure distribution, respectively; dimensionless, Eqs. (35–38)
$h, \bar{h}, \bar{h}'$ = enthalpy; $\bar{h} = h/h_s$; $\bar{h}' = (1 - \bar{h})/(1 - \bar{h}_w)$
M = Mach number
n = profile exponent, Eq. (9)
q = convective heat-transfer rate; also dynamic pressure
q_{FM} = free-molecule heat-transfer rate, Eq. (1)
q_{oc} = continuum heat-transfer rate with no mass transfer; Eq. (22) is one of several forms that can be used to evaluate q_{oc}
$q_{oc\ (\text{vort}=0)}$ = q_{oc} without vorticity; Eq. (22) can be used with $C_{\text{vort}} = 0$
q_{oo} = convective heat transfer rate with no mass transfer, bridged between q_{FM} and q_{oc}, Eq. (18)
$q_{\psi c}$ = continuum heat-transfer rate with mass transfer, Eq. (17)
$q_{\psi w}$ = convective heat-transfer rate with mass transfer, bridged between q_{FM} and $q_{\psi c}$, Eq. (14)
r_1, r_2 = radius of inner, outer cylinder, respectively, in Couette flow, Fig. 6
R = nose radius
Re, Re_s = Reynolds number and stagnation value, Eq. (23)
Y = coordinate normal to surface (positive inward) with origin in boundary layer, Fig. 1
z = dummy variable
α = angle of attack
$\gamma(z_1, z_2)$ = incomplete gamma function, Eq. (11)
$\Gamma(z)$ = gamma function, Eq. (12)
δ = increment, e.g., in Eq. (2)
δX = mass fraction, dimensionless
Δ_D, Δ_q = characteristic boundary-layer thicknesses for drag and heat transfer, respectively
λ = mean free path
μ = viscosity
ρ = density; $\rho_{21} \equiv \rho_2/\rho_\infty$
τ = shear
ψ = convective heat blockage factor, dimensionless, Eq. (17); $\bar{\psi}$ = modified ψ, Eqs. (19) and (20)

Subscripts

c, FM = continuum and free molecule, respectively
s, w = stagnation and wall, respectively
o = no mass transfer
$2, \infty$ = behind normal shock and freestream, respectively

Received April 2, 1970; revision received October 30, 1970.
* Research Scientist. Associate Fellow AIAA.

Introduction

IN atmospheric entry flights, a vehicle flies initially through a free-molecule atmosphere, passes through a transitional regime, and usually ends its flight in the continuum regime of gas dynamics. The physics of flight in the free-molecule and the continuum regimes has been reasonably well worked out, but in the transitional regime, where the physical situation is very complicated, the mathematical laws are not well established. This paper presents simple engineering methods of calculation (bridging formulas) for heat transfer, shear, and drag in the transitional regime. Equations also are proposed for lift and pressure distribution. The equations (which can be considered as semiempirical) were originally developed for the analysis of tektite entries,[1,2] but they are applicable to any blunt vehicle. The formulas for heat transfer and shear are derived from a simple kinetic theory model for a stagnation region on an axisymmetric blunt body, but they should furnish reasonable engineering approximations for other frontal locations on a blunt vehicle. The equations yield monotonic variations of the quantities solved for in the transitional regime. They are not particularly recommended for pointed bodies, especially near the leading edge; experiments with these bodies have indicated that some quantities overshoot in the transition regime, rather than approach from below both the free-molecule and the continuum asymptotes (e.g., Ref. 3).

Convective Heat-Transfer Bridging

A simple first-collision model is used. It is assumed that a typical packet of free molecules enters the boundary layer, makes a first collision with molecules already there, and the free molecules then become part of the continuum boundary layer with average energy equal to the energy in the boundary layer at the point of collision. The energy given up by the free molecules in the collisions is assumed to be ultimately received by the wall through successive collisions and finally

by impact with the wall, since there is no accumulation of energy in a quasi-steady-state boundary layer. We define an effective collision thickness Δ_q outside which collisions have a negligible effect on wall heat transfer, but inside which the heat transfer will be influenced; Δ_q is thus a kind of boundary-layer thickness. The coordinate system for this model is shown in Fig. 1, the ordinate being $\bar{h} = h/h_s$.

For free-molecule heat transfer in a stagnation region we can write

$$q_{FM} = A_{cq}(\rho_\infty V_\infty)h_s(1 - \bar{h}_w) \tag{1}$$

where A_{cq} is the accommodation coefficient which is assumed to be approximately unity. Then, for a small packet of molecules entering the boundary layer and making its first collision, we have, according to our model:

$$\delta q_{FM} = [h_s A_{cq}\rho_\infty V_\infty]\delta X(1 - \bar{h}) \tag{2}$$

where δX = mass fraction of molecules that make the first collision between Y and $Y + dY$ (or $\bar{h}$ and $\bar{h} + d\bar{h}$), and δq_{FM} is the heat given up by δX and eventually received at the wall; and we have assumed that A_{cq} is essentially the same for molecular collisions and wall collisions. From kinetic theory [see Ref. 4, Eq. (103–7)], we can evaluate δX as

$$\delta X = e^{-Y/\lambda}\,(dY/\lambda) \tag{3}$$

where the mean free path λ is an averaged value for the boundary layer. According to our model, we can write

$$q_{\psi w} = \sum_{\text{all } \delta X} \delta q_{FM} \tag{4}$$

$$\frac{q_{\psi w}}{h_s A_{cq}\rho_\infty V_\infty} = \frac{\sum_{\text{all } \delta X} \delta q_{FM}}{h_s A_{cq}\rho_\infty V_\infty} = \sum_{\text{all } \delta X} \delta X(1 - \bar{h}) \tag{5}$$

and using Eqs. (1) and (3),

$$q_{\psi w} = [q_{FM}/(1 - \bar{h}_w)] \int_{\text{all } \delta X} (1 - \bar{h})e^{-Y/\lambda}(dY/\lambda) \tag{6}$$

We now use

$$\bar{h}' = (1 - \bar{h})/(1 - \bar{h}_w) = f[Y/\Delta_q] \tag{7}$$

where $\bar{h}'(0) \approx 0$ and $\bar{h}'(1) = 1$ (as seen in Fig. 1). We now have

$$q_{\psi w} = q_{FM}\left[\int_0^{\Delta_q} \bar{h}'e^{-Y/\lambda}(dY/\lambda) + e^{-\Delta_q/\lambda}\right] \tag{8}$$

The last term in Eq. (8) accounts for heat transfer from molecules whose free path is greater than Δ_q; these molecules make their first effective collision with the wall.

To integrate Eq. (8), we require a functional form for $\bar{h}'$, as indicated in Eq. (7). We want to approximate the type of profile that we expect to have (Fig. 1), and also satisfy the requirements $f(0) \approx 0$ and $f(1) = 1$. This can be done with a polynomial (discussed below), and the simplest form with one term will be used.

$$\bar{h}' = (Y/\Delta_q)^n \tag{9}$$

where $n \geq 1$. The integration of Eq. (8) then yields

$$q_{\psi w}/q_{FM} = n(\lambda/\Delta_q)^n\gamma[n,(\Delta_q/\lambda)] \tag{10}$$

where γ is the incomplete gamma function[5] defined as

$$\gamma[n,(\Delta_q/\lambda)] = \int_0^{\Delta_q/\lambda} e^{-z}z^{n-1}dz \tag{11}$$

We recognize that λ/Δ_q is a type of Knudsen number. To consider a variation in the ratio λ/Δ_q we can visualize a change in ρ_∞. Since $\lambda \propto \rho_\infty^{-1}$, and Δ_q (being a kind of boundary-layer thickness) varies as $\rho_\infty^{-1/2}$, so $\lambda/\Delta_q \propto \rho_\infty^{-1/2}$. In the free-molecule limit, λ/Δ_q becomes very large, and in the continuum limit very small. In the free-molecule regime, $q_{\psi w}/q_{FM} \to 1$ in Eq. (10) as it should. In the continuum regime, as Δ_q/λ becomes large, the value of the incomplete gamma function approaches the value of the ordinary (complete) gamma function in Eq. (10). At the same time, $q_{\psi w}$ must approach $q_{\psi c}$. So, using the gamma function

$$\Gamma(n) = \int_0^\infty e^{-z}z^{n-1}dz \tag{12}$$

we write

$$q_{\psi c}/q_{FM} = n[\lambda/\Delta_q]^n\Gamma(n) \tag{13a}$$

$$\Delta_q/\lambda = \{[\Gamma(n + 1)](q_{FM}/q_{\psi c})\}^{1/n} \tag{13b}$$

The quantities q_{FM} and $q_{\psi c}$ in Eq. (13) are calculated for the same given conditions, and Δ_q must be assigned the value that satisfies Eq. (13b). When we substitute this evaluation into Eq. (10), we have a bridging equation,

$$q_{\psi w}/q_{\psi c} = [1/\Gamma(n)]\gamma\{n,[\Gamma(n + 1)(q_{FM}/q_{\psi c})]^{1/n}\} \tag{14}$$

Equation (14) is a monotonic function of $q_{FM}/q_{\psi c}$ and has the correct free-molecule and continuum asymptotes. The derivation has been performed essentially from the free-molecule end, and the agreement with the continuum end is forced. The function allows for no overshoot above the values of either q_{FM} or $q_{\psi c}$ as calculated for the same given conditions. The selection of n to fit available data will be discussed below.

In Fig. 2 are curves of Eq. (14) for $n = 1$, 1.25, 1.5, and 2. (Coordinates also shown on the figure include heat-transfer rates without mass transfer and surface shear values as given hereinafter.) Increasing the value of n in Eq. (14) tends to flatten the bridging curve in Fig. 2 downward. For non-

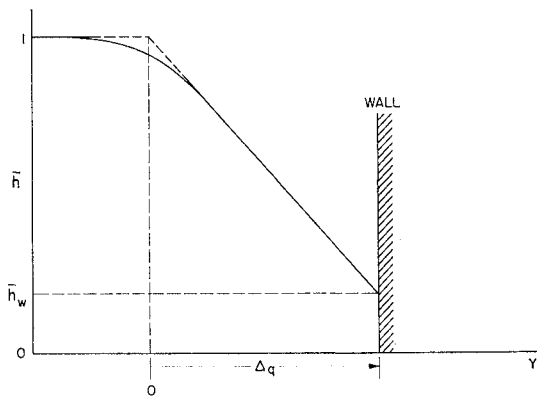

Fig. 1 Coordinate system used for heat-transfer bridging; Δ_q = effective collision thickness, an unspecified characteristic boundary-layer thickness.

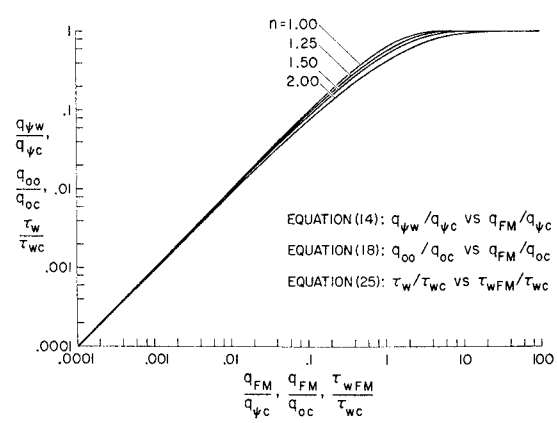

Fig. 2 General bridging relation for heat transfer and wall shear; variation with exponent n.

integer values of n (other than those plotted), the evaluation of Eq. (14) requires use of a table of incomplete gamma functions as in Ref. 5. For integer values of n, Eq. (14) can be evaluated in closed form; e.g.,

$$n = 1,\ q_{\psi w}/q_{\psi c} = 1 - e^{-(q_{FM}/q_{\psi c})} \tag{15}$$

$$n = 2,\ q_{\psi w}/q_{\psi c} = 1 - e^{-(2q_{FM}/q_{\psi c})^{1/2}}\left[1 + (2q_{FM}/q_{\psi c})^{1/2}\right] \tag{16}$$

It will be shown below that the simple linear form, using $n = 1$, yields engineering accuracy for the boundary-layer cases investigated, the agreement being best for the supersonic (or hypersonic) case.

Instead of using Eq. (9), it is also possible to represent $\bar{h}'$ as a finite polynomial summation of terms of this type multiplied by coefficients and with integer exponents. However, this more complicated evaluation is probably not justified in view of the approximations already made.

Equation (14) is considered to be valid with or without mass transfer when $q_{\psi c}$ is given its appropriate value with or without mass transfer. Let us define the heat blockage factor for continuum heat transfer as

$$\psi = q_{\psi c}/q_{oc} \tag{17}$$

With no ablation, $\psi = 1$ and Eq. (14) specializes to

$$q_{oo}/q_{oc} = [1/\Gamma(n)]\gamma\{n,[\Gamma(n+1)(q_{FM}/q_{oc})]^{1/n}\} \tag{18}$$

where q_{oo} is the bridged heat-transfer value for the no-blowing case. Equation (18) is functionally identical with Eq. (14), so it is also in Fig. 2. For the ablation case, we can consider that ψ operates on q_{oc} but not on q_{FM}, and we can define a modified heat blockage factor $\bar{\psi}$ as

$$\bar{\psi} = q_{\psi w}/q_{oo} \tag{19}$$

When we substitute the evaluations in Eqs. (14, 17, and 18) into Eq. (19), we obtain

$$\bar{\psi} = \frac{\psi\gamma\{n,[\Gamma(n+1)(q_{FM}/\psi q_{oc})]^{1/n}\}}{\gamma\{n,[\Gamma(n+1)(q_{FM}/q_{oc})]^{1/n}\}} \tag{20}$$

Equations (18–20) are alternate (but equivalent) forms of our heat-transfer bridging relations. The quantities q_{oo} and $\bar{\psi}$ are mainly of conceptual interest, but may be preferred for some calculations. For the case with $n = 1$, Eq. (18) specializes to the form of Eq. (15), and Eq. (20) specializes to

$$\bar{\psi} = \psi(1 - e^{-q_{FM}/\psi q_{oc}})/(1 - e^{-q_{FM}/q_{oc}}) \tag{21}$$

The foregoing analysis is an approximation begun from a simple model. The type of bridging relationship obtained is a mathematical consequence of the selection of the model. Bridged heat-transfer values can be calculated using Eq. (14) or (15) or read from Fig. 2. Within the framework of approximations made, the simplest choice of n to be investigated is unity. This value is suggested for stagnation region boundary layers under high-speed conditions, because the enthalpy profile is approximately linear near the body surface. (Molecular collisions near the wall have the greatest effect on heat transfer, so this portion of the boundary layer is the most important in the analysis.)

Some comparisons of the calculated bridging relations with experiment are available for the case with no mass transfer. Experimental measurements of heat transfer in supersonic flows from Fig. 5 of Ref. 6 are plotted in Fig. 3; these are compared with the calculated values of the continuum heat transfer, the free-molecule heat transfer, and the bridged heat transfer value obtained from Eq. (15) ($n = 1$). The data shown are stagnation-point heat-transfer measurements on a spherical body at nominal Mach numbers of 5.7 and 8 with stagnation temperatures of 2100° and 2300°R. We calculate q_{FM} from Eq. (1) with A_{eq} taken as 0.8 (as suggested by tabulated values in Ref. 7). A form of the heat transfer equation as given in Ref. 8 (see also Refs. 1 and 2) is

$$q_{oc} = C_{cal}(\rho_\infty/R)^{1/2}(h_s)^{1.575}(1 - \bar{h}_w) \times \left[1 + \frac{C_{vort}}{[\rho_\infty R(h_s)^{1/2}]^{1/2}}\right] \tag{22}$$

where the calorimeter constant C_{cal} is taken as 0.594 $g^{1.075}$ sec^{-1} $cal^{-0.575}$, the vorticity correction constant C_{vort} is 0.628×10^{-3} $cal^{1/4}$ $g^{1/4}$ cm^{-1}, and the other units are q_{oc} = cal/cm²-sec, ρ_∞ = g/cm³, R = cm, h_s = cal/g. The quantities plotted in Fig. 3 are normalized by dividing by $q_{oc(vort=0)}$, which is obtained from Eq. (22) by setting C_{vort} 0. The Re_s is based on the flight enthalpy and stagnation conditions at the model, as originally used in Ref. 6. Thus,

$$Re_s = 9150(h_s)^{1/2}\rho_{s\infty}R/\mu_s \tag{23}$$

The factor 9150 is $(2J)^{1/2}$ in $erg^{1/2}$ $cal^{-1/2}$, J being the mechanical equivalent of heat, and the units are as in Eq. (22) with μ_s = poise. As shown in Fig. 3, the calculated bridging obtained from Eq. (15) checks quite well with these experimental measurements. Some other supersonic heat transfer measurements are in Fig. 9 of Ref. 9, and comparison with these measurements is also satisfactory (not shown). The referenced figure also shows calculations valid over part of the transition regime and a good comparison over the whole regime with H. K. Cheng's thin shock-layer analysis.

A comparison of calculated bridging with measurements of heat transfer in subsonic flows is shown in Fig. 4. The data, which are from Fig. 9c of Ref. 10, are stagnation region heat transfer measurements from spheres. Curves from Fig. 2 are replotted in Fig. 4 with three values of n; $n = 1.5$ gives the best agreement with the measurements. Also shown is a form of Sherman's equation,[10] which fits the data well. Sherman describes this equation as a simple algebraic formula

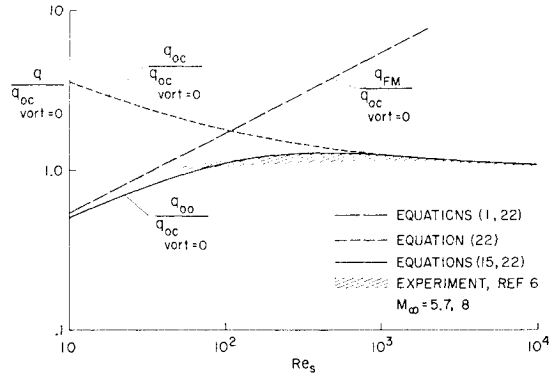

Fig. 3 Comparison of calculated and measured heat transfer for spheres in supersonic flows without mass transfer.

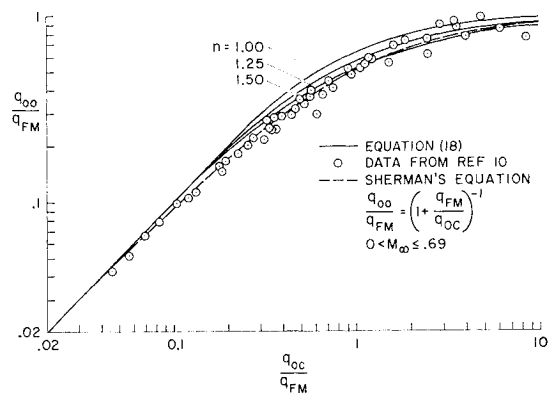

Fig. 4 Comparison of calculated and measured heat transfer for spheres in subsonic flows without mass transfer.

that gives an adequate fit to the entire transition process for some subsonic experiments; it is essentially equivalent to the Yang-Lees equation for wall shear in Couette flow (see Fig. 6).

Based on the comparisons made, it is recommended that heat-transfer bridging for supersonic or hypersonic flows (the important application) should be obtained from Eq. (15) ($n = 1$). For subsonic flows, Eq. (14) with $n = 1.5$ is best, although a reasonable engineering approximation can still be obtained with $n = 1$ (or, alternatively, Sherman's equation can be used). The following empirical evaluation for n for heat transfer can be proposed:

$$n = 1 + 0.5e^{-M_\infty} \tag{24}$$

Although the bridging relations are derived for a stagnation region, they should furnish good approximations for other frontal locations on a blunt body when the continuum and free-molecule heat transfer rates are evaluated for the particular location. The comparisons with experimental heat transfer rates have been made for cases without mass transfer. The bridging relations given should be valid approximations for the general case with mass transfer, since the no-mass-transfer case is simply a specialization, and the bridging relations will have the correct asymptotes for the general case. Experimental verification for the case with mass transfer would be desirable.

Surface Shear Bridging

To calculate surface shear in the transitional regime, we use the same first collision model as that used for convective heat transfer, except that we now consider the transfer of x momentum rather than energy. The derivation, essentially for the stagnation region of a blunt body, completely parallels the development for heat-transfer bridging, and the resulting shear bridging equation is identical in form to Eq. (14). Thus,

$$\tau_w/\tau_{wc} = [1/\Gamma(n)]\gamma\{n,[\Gamma(n+1)(\tau_{wFM}/\tau_{wc})]^{1/n}\} \tag{25}$$

With $n = 1$ we have [equivalent to Eq. (15)]

$$\tau_w/\tau_{wc} = 1 - e^{-(\tau_{wFM}/\tau_{wc})} \tag{26}$$

Equations (25) and (26) are the functions shown in Fig. 2. The continuum shear τ_{wc} is considered to be the value for the general case with mass transfer. In calculating it, a mass addition factor (ψ_τ) for shear should be applied to the calculated no-mass-transfer value of continuum shear. Alternative bridging forms analogous to the development in Eqs. (18–21) can be written for the wall shear, but will not be given here.

Experimental data were not found for the most desirable comparison case that would consist of measurements of wall shear in a stagnation region in hypersonic flow (preferably both with and without mass transfer). Comparisons of calculated and measured wall shears have been made, however, for the flat plate in subsonic flow (Fig. 5) and for low-speed Couette flow (Fig. 6). In Fig. 5 the data are from Fig. (9a) of Ref. 10, and the calculated shears were obtained from Eq. (26) using $n = 1$, which gave the best fit to the experimental data; the agreement obtained is quite satisfactory. In Fig. 6, the measured data are from Fig. 11 of Ref. 11, and the calculations were made using Eq. (25) with $n = 1.5$, the best-fit value. Calculations using $n = 1$ (not shown) yielded shear values up to 15% high in the midtransition range, although both asymptotes were necessarily correct. Thus, shear in Couette flow can be successfully calculated using Eq. (25) with a selected value of n, although Couette flow is quite different from an unbounded flow in a stagnation region which was used as the model in obtaining Eq. (25). The Couette flow is one of the rare examples for which rigorously evaluated shear (and heat transfer) through the transitional regime have been derived; the Yang-Lees equation for Couette flow shear is also shown in Fig. 6.

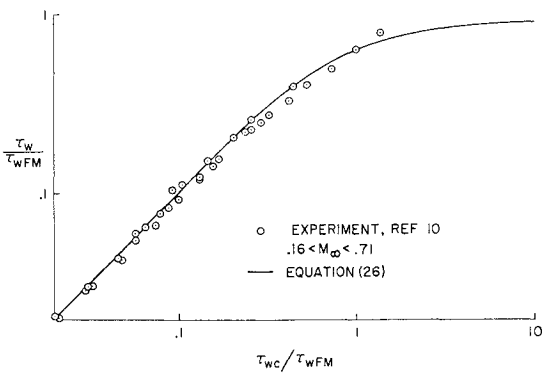

Fig. 5 Comparison of calculated surface shear bridging with measured surface shear for subsonic flat plate (without mass transfer).

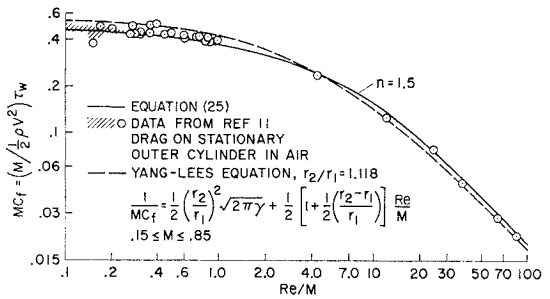

Fig. 6 Comparison of calculated surface shear bridging with measured surface shear in low-speed Couette flow.

Drag Bridging

A bridging relation for C_D is often necessary for calculations of entry flights, since C_D must initially have a free-molecule value and, for many entries, the final value of C_D will be the continuum value. Here we make use of our first-collision model. The approximation considers a two-fluid flow, and we assume that collisions occurring outside of Δ_D, a kind of boundary layer thickness, have a negligible effect on drag, while collisions occurring within Δ_D affect the drag. The molecules (first fluid) that have a longer free path than Δ_D are considered to make their first effective collision with the body and contribute to free-molecule drag. The other molecules (second fluid) make collisions with each other within the depth Δ_D; these molecules bathe the body in a continuum fluid and contribute to continuum drag. An attempt at a more rigorous development would require that Δ_D vary with position on the body, but we will take Δ_D to be some average value for the whole body. Similarly, λ for molecules near the body will depend on position on the body, but we will use a nominal or averaged mean free path λ_2 for the gas between the shock wave and the body. We again consider that the body is blunt.

According to our model, we can sum the free-molecule and continuum drags and obtain

$$C_D q_\infty A = C_{DFM} q_{\infty FM} A + C_{Dc} q_{\infty c} A \tag{27a}$$

$$C_D = C_{DFM} q_{\infty FM}/q_\infty + C_{Dc} q_{\infty c}/q_\infty \tag{27b}$$

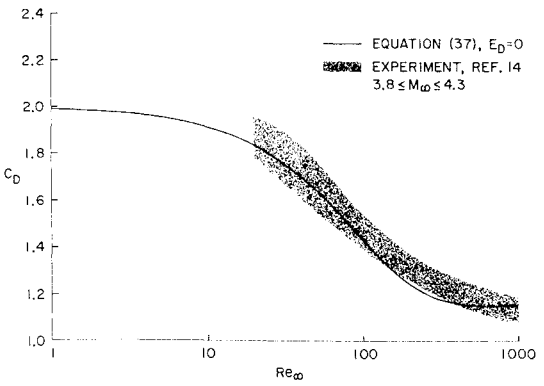

Fig. 7 Comparison of calculated and measured values of the drag coefficient for spheres in the transitional regime.

The dynamic pressure ratios are evaluated as density or mass fraction ratios:

$$q_{\infty FM}/q_\infty = \rho_{\infty FM}/\rho_\infty = e^{-\Delta_D/\lambda_2} \tag{28a}$$

$$q_{\infty c}/q_\infty = \rho_{\infty c}/\rho_\infty = 1 - e^{-\Delta_D/\lambda_2} \tag{28b}$$

Combining Eq. (28) with (27b), we have

$$C_D = C_{D_c} + (C_{DFM} - C_{D_c})e^{-\Delta_D/\lambda_2} \tag{29}$$

For convenience we define

$$G_D = (C_{DFM} - C_{D_c})/C_{D_c} \tag{30}$$

and we have

$$C_D = C_{D_c}(1 + G_D e^{-\Delta_D/\lambda_2}) \tag{31}$$

we have developed C_D as a function of Δ_D/λ_2, which is a reciprocal Knudsen number. We observe, also, that Eqs. (29) and (31) have the correct asymptotes. To this point the preceding derivation is similar to those found in Refs. 12 and 13, but from a somewhat different point of view. In Ref. 12, the equivalent of Δ_D is specified as the shock standoff distance, evaluated empirically in terms of ρ_{21} and R for a sphere; the reciprocal Knudsen number obtained is then multiplied by a constant factor to give drag coefficients that fit experimental data.

We postulate a functional form for Δ_D as $\Delta_D = f_\alpha(R, Re_\infty, M_\infty$, gas, α, body shape) and from dimensional considerations, we write $\Delta_D = Rf_\beta(Re_\infty, M_\infty$, gas, α, body shape) where the nose radius R characterizes the body size. We can write $\Delta_D = (R/\rho_{21})(\rho_{21}f_\beta)$ and when we let $f_\gamma = \rho_{21}f_\beta$, we have

$$\Delta_D = Rf_\gamma/\rho_{21} \tag{32}$$

where $f_\gamma = f_\gamma(Re_\infty, M_\infty$, gas, α, body shape). Equation (32) has the form of an approximate calculation for the shock standoff distance for a sphere, and (as one can infer from Ref. 12), it is logical to assume that Δ_D should relate to the shock standoff distance. We may assume that f_γ has little dependence on the particular gas. We also assume that for hypersonic flows f_γ will approach an approximate limiting value f_Δ where $f_\Delta = f_\Delta(\alpha$, body shape). We now write

$$\Delta_D/\lambda_2 = R\rho_\infty f_\Delta/\lambda_2\rho_2 \tag{33}$$

This is the form of the exponent in Ref. 12 where f_Δ (in that case) would have a constant value for a sphere. As described in Ref. 12, this exponent gives good correlations with available data.

For many flight cases, body shape does not change much in the passage through the transitional regime, and it seems reasonable to approximate f_Δ as a constant. Also, for a particular gas, $\lambda_2\rho_2$ can be approximated as a constant (although it will be different for different gases). We now define a new constant,

$$C_\Delta = f_\Delta/\lambda_2\rho_2 \tag{34}$$

which can depend somewhat on flight conditions but should depend mainly on body shape, angle of attack, and the particular gas in which flight is occurring. For convenience, instead of C_Δ, we will use the constant E_D defined by,

$$C_\Delta = 15 \times 10^6(1 + E_D) \tag{35}$$

The drag bridging exponent is now

$$\Delta_D/\lambda_2 = 15 \times 10^6(R\rho_\infty)(1 + E_D) \tag{36}$$

and our drag bridging Eq. (31) is

$$C_D = C_{D_c}[1 + G_D e^{-15\times 10^6(R\rho_\infty)(1+E_D)}] \tag{37}$$

The constant 15×10^6 in Eqs. (35–37) was determined by setting $E_D = 0$ and matching calculated values of drag with the measured drag data for spheres in air of Ref. 14. The units are R, cm and ρ_∞, g/cm^3. Figure 7 shows that with the selection of one constant E_D, a good fit is obtained over a wide range of data, and Eq. (37) has a reasonable functional form. The data of Ref. 14 were obtained in air at a nominal settling chamber temperature of 300°K over a Mach number range of 3.8–4.3. These data indicate that, at high speeds, any M effect on the transition of C_D is probably small. Using $E_D = 0$, a good fit was also obtained with sphere drag data in air reported in Ref. 12 (not shown). These latter data were obtained in hypersonic flows in dissociated and undissociated air. Another set of sphere drag data obtained in helium is reported in Ref. 12. Because $\lambda_2\rho_2$ is different for helium than for air, a value of $E_D \approx 2$ in Eq. (37) is needed to give the best fit to these data.

We can adjust E_D, in principle, to account approximately for the effects of all the variables which can affect Δ_D/λ_2 (during passage through the transitional regime). Unless data are at hand, E_D would normally be assigned the value zero as for a sphere in supersonic flow in air. Although the (presumably modest) dependence of E_D on body shape may not be accurately known, the values of C_D calculated from Eq. (37) will also depend directly on body shape through C_{D_c} and G_D.

Lift and Pressure Distribution

The development leading to Eq. (37) can be performed for C_L, and one can propose, as a reasonable approximation for blunt bodies,

$$C_L = C_{L_c}[1 + G_L e^{-15\times 10^6(R\rho_\infty)(1+E_L)}] \tag{38}$$

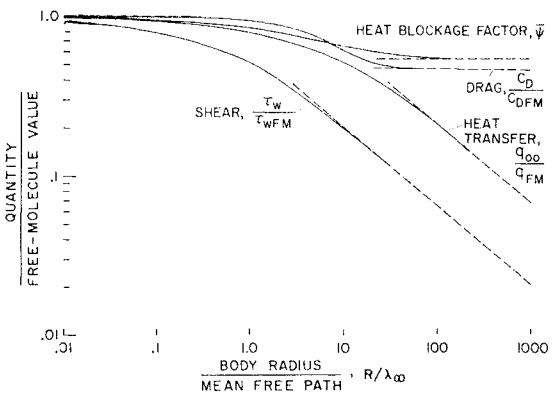

Fig. 8 Representative calculation of bridging between free-molecule and continuum flow.

where

$$G_L = (C_{LFM} - C_{Lc})/G_{Lc} \quad (39)$$

and with R in cm and ρ_∞ in g/cm^3.

The constant 15×10^6 could be subject to adjustment in combination with E_L. Lacking firm data, one would suggest taking E_L equal to E_D for a given body shape. Using the same constants means that the transition of lift and drag will follow similar functional curves. A special case, wherein the lift/drag ratio is to be constant over the entire spectrum, further would require that G_L be equal to G_D.

The derivation for drag bridging (and lift) is an approximation that makes use of quantities that are, in effect, averaged over a body. The pressure on a body is, of course, a local quantity which varies over the body. However, as a first approximation for the bridging of pressure on a blunt body, one can again propose the use of Eqs. (30) and (37) with pressure (or its coefficient) inserted in place of the drag coefficients and with E_p a function of position on the body. In the absence of data, one would also use the same constants as for drag calculations, 15×10^6 and $E_p = E_D$. The use of the drag constants is equivalent to the assumption that the pressure transition, everywhere on the body, proceeds at the same rate as the drag transition. Whatever error is introduced by this approximation should be reasonably well-bounded if one has good values for the free-molecule and continuum regime asymptotes of the local pressures.

Example of Free-Molecule-Continuum Bridging

Representative curves for the bridging relationships presented are shown in Fig. 8. The ordinate quantities, normalized to their free-molecule values, are plotted against a reciprocal Knudsen number. The dotted lines on the right side of the figure are the continuum-regime asymptotes for the several quantities, while on the left side the free-molecule asymptote for all quantities is unity. Although the bridging equations are general, the inputs to the equations, and therefore the curves obtained, will depend on the individual case calculated. The curves in the figure are from a tektite entry calculation, and $n = 1$ was used for the heat transfer and shear bridgings. A curve for $q_{\psi w}$ [Eq. (15)] is not shown; this quantity is the product of $\bar{\psi}$ and q_{∞} [Eq. (19)], for which the curves are shown. It is noted that the various quantities approach their asymptotes at different rates. (Under some conditions, one can consider that all of the quantities plotted are not even in the same regime.) The figure illustrates an important feature of the bridging relations presented. They automatically place control of the various calculated quantities in the appropriate controlling regime, the free-molecule, transitional, or continuum. This means that if the value of a calculated quantity is close to the value of the corresponding free-molecule quantity, it is considered to be in the free-molecule regime (and similarly for the continuum regime). If the value of a calculated quantity is close to neither the corresponding free-molecule nor the continuum value, it is considered to be in the transitional regime.

Curves corresponding to those of Fig. 8 can be plotted for other materials, and most of the curves will be similar, but somewhat displaced. The heat-transfer curve (without mass transfer) is approximately universal; the drag curve is influenced mainly by body shape; the other curves (shear and heat blockage factor) will vary somewhat with relative rates of mass transfer of the material that is being considered.

Conclusions

The bridging relations presented are recommended as engineering approximations for blunt bodies, to be used in cases for which more rigorously developed specific relations do not exist. The heat transfer and shear equations are to be used for frontal locations that can be seen by the oncoming flow. The equations recommended are: heat transfer, supersonic, Eq. (15); heat transfer, subsonic, Eq. (14) with $n = 1.5$, or if a simpler but cruder approximation is adequate, Eq. (15), or Sherman's equation (see Fig. 4); shear in unbounded flows, Eq. (26); drag, Eq. (37); if E_D is unknown, let $E_D = 0$; lift, Eq. (38); if E_L is unknown, let $E_L = 0$; and pressure, an equation form similar to Eq. (37).

The equations presented are considered to be restricted in use to blunt type body shapes, because the equations are functionally monotonic and do not yield overshoots (which may occur with sharp or slender bodies). The structure of the equations insures that they have the correct asymptotes, which tends to put a bound on inaccuracies when used for blunt bodies.

References

[1] Matting, F. W. and Chapman, D. R., "Generalized Ablation Analysis with Application to Heat-Shield Materials and Tektite Glass," AIAA Paper 65-490, San Francisco, Calif., 1965.

[2] Matting, F. W. and Chapman, D. R., "Analysis of Surface Ablation of Noncharring Materials with Description of Associated Computing Program," TN D-3758, 1966, NASA.

[3] Vidal, R. J. and Bartz, J. A., "Experimental Studies of Low-Density Effects in Hypersonic Wedge Flows," Advances in Applied Mechanics, Supplement 3, Vol. I, 1965, *Rarefied Gas Dynamics*, Fourth Symposium, edited by J. H. de Leeuw, Academic Press, New York, pp. 467–486.

[4] Page, L., *Introduction to Theoretical Physics*, 2nd ed., Van Nostrand, N.Y., 1935.

[5] Abramowitz, M. and Stegun, I. A., *Handbook of Mathematical Functions with Formulas, Graphs, and Mathematical Tables*, U.S. Department of Commerce, National Bureau of Standards Applied Mathematics Series 55, Washington, D.C., June 1964.

[6] Ferri, A. and Zakkay, V., "Measurements of Stagnation Point Heat Transfer at Low Reynolds Numbers," *Journal of the Aerospace Sciences*, Vol. 29, No. 7, July 1962, pp. 847–850.

[7] Kennard, E. H., *Kinetic Theory of Gases*, McGraw-Hill, New York, 1938.

[8] Detra, R. W., Kemp, N. H., and Riddell, F. R., "Addendum to Heat Transfer to Satellite Vehicles Reentering the Atmosphere," *Jet Propulsion*, Vol. 27, No. 12, Dec. 1957, pp. 1256–1257.

[9] Cheng, H. K., "Viscous Hypersonic Blunt-Body Problems and the Newtonian Theory," *Proceedings of the International Symposium on Fundamental Phenomena in Hypersonic Flow*, edited by J. Gordon Hall, 1966, Cornell University Press, Ithaca, N.Y., pp. 90–132.

[10] Sherman, F. S., "A Survey of Experimental Results and Methods for the Transition Regime of Rarefied Gas Dynamics," Advances in Applied Mechanics, Supplement 2, Vol. II, 1963, *Rarefied Gas Dynamics*, Third Symposium, edited by J. A. Laurmann, Academic Press, New York, pp. 228–260.

[11] Yang, H.-T. and Lees, L., "Plane Couette Flow at Low Mach Number According to the Kinetic Theory of Gases," *Proceedings of the Fifth Midwestern Conference on Fluid Mechanics*, The Engineering Research Institute, 1957, pp. 41–65.

[12] Masson, D. J., Morris, D. N., and Bloxsom, D. E., "Measurements of Sphere Drag from Hypersonic Continuum to Free-Molecule Flow," Advances in Applied Mechanics, Supplement 1, 1961, *Rarefied Gas Dynamics*, Second Symposium, edited by L. Talbot, Academic Press, New York, pp. 643–661.

[13] Rott, N. and Whittenbury, C. G., "A Flow Model for Hypersonic Rarefied Gas Dynamics with Applications to Shock Structure and Sphere Drag," Rept. SM-38524, May 1961, Douglas Aircraft.

[14] Wegener, P. P. and Ashkenas, H., "Wind Tunnel Measurements of Sphere Drag at Supersonic Speeds and Low Reynolds Numbers," *Journal of Fluid Mechanics*, Vol. 10, Pt. 4, June 1961, pp. 550–560.